The Rab21-GEF activity of Varp, but not its Rab32/38 effector function, is required for dendrite formation in melanocytes

Norihiko Ohbayashi*, Ayaka Yatsu*, Kanako Tamura*, and Mitsunori Fukuda
Laboratory of Membrane Trafficking Mechanisms, Department of Developmental Biology and Neurosciences, Graduate School of Life Sciences, Tohoku University, Aobayama, Aoba-ku, Sendai, Miyagi 980-8578, Japan

ABSTRACT **Vacuolar protein sorting 9 (VPS9)–ankyrin-repeat protein (Varp) has recently been identified as an effector molecule for two small GTPases—Rab32 and Rab38—in the transport of a melanogenic enzyme tyrosinase-related protein 1 (Tyrp1) to melanosomes in melanocytes. Although Varp contains a Rab21–guanine nucleotide exchange factor (GEF) domain (i.e., VPS9 domain), since Rab21-GEF activity is not required for Tyrp1 transport, nothing is known about the physiological significance of the Rab21-GEF activity in melanocytes. Here we show by knockdown-rescue experiments that the Rab21-GEF activity of Varp, but not its Rab32/38 effector function, is required for forskolin-induced dendrite formation of cultured melanocytes. We found that Varp-deficient cells are unable to extend dendrites in response to forskolin stimulation and that reexpression of wild-type Varp or a Rab32/38-binding–deficient mutant Varp(Q509A/Y550A) in Varp-deficient cells completely restores their ability to form dendrites. By contrast, VPS9 mutants (D310A and Y350A) and a vesicle-associated membrane protein 7 (VAMP7)-binding–deficient mutant were unable to support forskolin-induced dendrite formation in Varp-deficient cells. These findings indicate that the Rab21-GEF activity and Rab32/38 binding activity of Varp are required for different melanocyte functions, that is, Rab21 activation by the VPS9 domain is required for dendrite formation, and the Rab32/38 effector function of the ankyrin repeat 1 domain is required for Tyrp1 transport to melanosomes, although VAMP7-binding ability is required for both functions.**

Monitoring Editor
Thomas F.J. Martin
University of Wisconsin

Received: Apr 14, 2011
Revised: Nov 8, 2011
Accepted: Dec 8, 2011

INTRODUCTION

The small GTPase Rab is a conserved membrane-trafficking protein that regulates a variety of intracellular membrane-trafficking events in all eukaryotic cells (reviewed in Schwartz *et al.*, 2007; Fukuda, 2008; Stenmark, 2009; Hutagalung and Novick, 2011). Rab is generally viewed as a molecular switch that functions by cycling between two nucleotide-bound states—a GDP-bound, inactive state and a GTP-bound, active state. Three key factors—a guanine nucleotide exchange factor (GEF), a Rab effector, and a GTPase-activating protein (GAP)—are generally believed to be required to exert the function of Rab protein in membrane trafficking (reviewed in Barr and Lambright, 2010). The GTP-bound, active form of Rab, which is activated by a specific GEF, promotes membrane trafficking through interaction with a specific effector molecule and is then inactivated by a specific GAP. Although these three factors are usually encoded by different genes, recent evidence indicates that some factors play bifunctional roles in Rab-mediated membrane trafficking (so-called Rab GEF/GAP cascades; reviewed in Stenmark, 2009). A well-characterized example of a Rab GEF cascade is Sec2p, which is an effector for Ypt31/32p and a GEF for Sec4p in the budding yeast *Saccharomyces cerevisiae* (Ortiz *et al.*, 2002). Ypt31/32p recruits Sec2p and then activates Sec4p on the secretory vesicles in budding yeasts. Similarly, a class C VPS/HOPS complex, which is a GEF for Rab7, interacts with Rab5

This article was published online ahead of print in MBoC in Press (http://www.molbiolcell.org/cgi/doi/10.1091/mbc.E11-04-0324) on December 14, 2011.

*These authors contributed equally to this work.

Address correspondence to: Mitsunori Fukuda (nori@m.tohoku.ac.jp).

Abbreviations used: ANKR, ankyrin repeat; EGFP, enhanced green fluorescent protein; Fsk, forskolin; GAP, GTPase-activating protein; GEF, guanine nucleotide exchange factor; IBMX, 3-isobutyl-1-methylxanthine; mStr, monomeric Strawberry; PKA, protein kinase A; shRNA, short hairpin RNA; siRNA, small interfering RNA; SR, siRNA resistant; Tyrp1, tyrosinase-related protein 1; VAMP7, vesicle-associated membrane protein 7; Varp, VPS9-ankyrin-repeat protein; VID, VAMP7-interaction domain; VPS9, vacuolar protein sorting 9.

and is required for Rab5-to-Rab7 (i.e., early endosome–to–late endosome) conversion (Rink *et al.*, 2005). An example of a Rab GAP cascade is Gyp1p, which specifically interacts with Ypt32p and also functions as a GAP for Ypt1p (Rivera-Molina and Novick, 2009). Gyp1p regulates a transition from a Ypt1p-positive compartment to a Ypt32p-positive compartment in budding yeasts. More recently, several Tre-2/Bub2/Cdc16-domain–containing proteins/putative Rab-GAPs have been shown to bind nonsubstrate Rabs via a domain other than their GAP domain (Fukuda *et al.*, 2008; Kanno *et al.*, 2010; reviewed in Fukuda, 2011), suggesting that Rab GAP cascades may be more common in Rab-mediated membrane-trafficking events.

Because the vacuolar protein sorting 9 (VPS9)–ankyrin-repeat protein (Varp; official name according to the National Center for Biotechnology Information, Ankrd27) molecule contains both a VPS9 domain (Carney *et al.*, 2006), which possesses Rab21-GEF activity (Zhang *et al.*, 2006), and a Rab32/38 effector domain (Wang *et al.*, 2008; Tamura *et al.*, 2009, 2011), Varp may participate in a Rab GEF cascade. However, nothing is known about the functional relationship between Rab21 and Rab32/38 in membrane trafficking. The Rab32/38 effector function of Varp has recently been shown to be required for the transport of tyrosinase-related protein 1 (Tyrp1) to melanosomes in melanocytes, but there is no evidence that the Rab21-GEF activity of Varp is required for this process (Tamura *et al.*, 2009, 2011). More recently, Varp and Rab21 have been shown to regulate neurite outgrowth of mouse hippocampal neurons and PC12 cells, but whether Rab32/38 is involved in this process has not been investigated (Burgo *et al.*, 2009). It would therefore be interesting to learn whether the VPS9 domain (i.e., the Rab21-GEF activity) and an ankyrin repeat 1 domain (ANKR1; i.e., the Rab32/38 effector activity) of Varp function independently or cooperatively.

In the present study, we used a knockdown-rescue approach combined with site-directed mutagenesis to investigate involvement of the Rab21-GEF activity and Rab32/38–binding activity of Varp in forskolin-induced dendrite formation of melanocytes. The results showed that a Rab32/38-binding–deficient mutant fully supported forskolin-induced dendrite formation of melanocytes but VPS9 mutants of Varp did not. We discuss the distinct mechanisms of Varp/Rab32/38–dependent Tyrp1 trafficking and Varp/Rab21–dependent dendrite formation in melanocytes based on our findings.

RESULTS

Varp is required for forskolin-induced dendrite formation in melanocytes

Varp was originally identified as a Rab21-GEF through its VPS9 domain (Zhang *et al.*, 2006), but recently it has been shown to function as a Rab32/38 effector in Tyrp1 transport in melanocytes (Tamura *et al.*, 2009, 2011). The physiological significance of the Rab21-GEF activity of Varp in melanocytes, however, had not been determined. To do so, we focused on forskolin-induced dendrite outgrowth of melanocytes (Passeron *et al.*, 2004), because dendrite formation of melanocytes is believed to be essential for efficient transfer of melanosomes from melanocytes to neighboring keratinocytes (reviewed in Seiberg, 2001; Van Den Bossche *et al.*, 2006), and Varp has recently been shown to be involved in neurite outgrowth of mouse hippocampal neurons and PC12 cells (Burgo *et al.*, 2009). When cultured mouse melanocytes (i.e., melan-a cells) were treated for 20 h with 20 μM forskolin (or DMSO alone as a control), the cells extended several dendrites and dramatically changed their shape from a bipolar shape to a dendritic shape (Figure 1A, left half). Of interest, knockdown of endogenous Varp molecules in melanocytes completely suppressed the forskolin-induced dendrite formation (Figure 1, A, right half, and B), indicating that Varp is involved in dendrite outgrowth of melanocytes, the same as in neurite outgrowth of hippocampal neurons (Burgo *et al.*, 2009). Similar Varp-dependent dendrite formation was also observed in cells treated with two other cAMP-elevating reagents, 8-bromo cAMP and 3-isobutyl-1-methylxanthine (IBMX; a phosphodiesterase inhibitor), although their dendrites were much shorter than the dendrites of forskolin-treated cells (Figure 1, C and D, respectively). Because forskolin-induced dendrite formation in melan-a cells was clearly suppressed by H-89 (a protein kinase A [PKA] inhibitor) but was not suppressed by wortmannin (a phosphatidylinositol 3 [PI3]-kinase inhibitor) or by U0126 (a mitogen-activated protein kinase kinase [MEK] inhibitor), a cAMP-PKA pathway must be involved in forskolin-induced dendrite formation in melan-a cells (Figure 2).

We also tested the effect of overexpression of Varp on dendrite formation in melan-a cells and, as expected, found that overexpression of Varp in melan-a cells treated with IBMX, a weak inducer of dendrite formation (Figure 1D), promoted dendrite formation, although it did not induce dendrite formation in the absence of IBMX (i.e., in the presence of DMSO alone; Figure 1E). Of interest, however, overexpression of Varp in melan-a cells treated with forskolin, a strong inducer of dendrite formation (Figure 1B), had no effect on dendrite formation (Supplemental Figure S1, A, right half, and B). This discrepancy may be explained by the possibility that Varp activation is insufficient in IBMX-treated cells (i.e., exogenously expressed Varp is able to contribute to dendrite formation), whereas activation of Varp is saturated in forskolin-treated cells (i.e., exogenously expressed Varp is unable to contribute to dendrite formation).

The Rab21-GEF activity of Varp is essential for dendrite formation in melanocytes

Because Varp consists of at least four domains—a VPS9/Rab21-GEF domain (Zhang *et al.*, 2006), an ANKR1/Rab32/38 effector domain (Wang *et al.*, 2008; Tamura *et al.*, 2009, 2011), a vesicle-associated membrane protein 7 (VAMP7)-interaction domain (VID; Burgo *et al.*, 2009), and an ANKR2 domain of unknown function (Figure 3)—we next attempted to determine the role of the first three domains in forskolin-induced dendrite formation of melanocytes. We did so by performing knockdown-rescue experiments with mutants of the three domains of Varp, each of which lacks the function of only one of the three domains (summarized in Figure 3; Tamura *et al.*, 2011). In brief, the two VPS9 mutants—Varp(D310A) and Varp(Y350A)—that we used lack a conserved key residue of the VPS9 domain for GEF activity (Delprato *et al.*, 2004; Delprato and Lambright, 2007; Tamura *et al.*, 2011); the ANKR1 mutant Varp(Q509A/Y550A) completely lacks Rab32/38–binding activity (Tamura *et al.*, 2011); and the Varp-ΔVID mutant lacks VAMP7-binding activity (Burgo *et al.*, 2009).

To determine the functional involvement of the Rab21-GEF activity of the VPS9 domain of Varp, we reexpressed each VPS9 point mutant of Varp^{SR} (small interfering RNA [siRNA]-resistant [SR] form) in Varp-deficient melanocytes (Figure 4). Although reexpression of wild-type Varp^{SR} in Varp-deficient cells clearly restored forskolin-induced dendrite formation (Figure 4A, second row from the top), neither VPS9 point mutant (D310A or Y350A) restored it at all (Figure 4, A, bottom two rows, and B), strongly indicating that the Rab21-GEF activity of Varp is essential for forskolin-induced dendrite formation in melanocytes. These results are in sharp

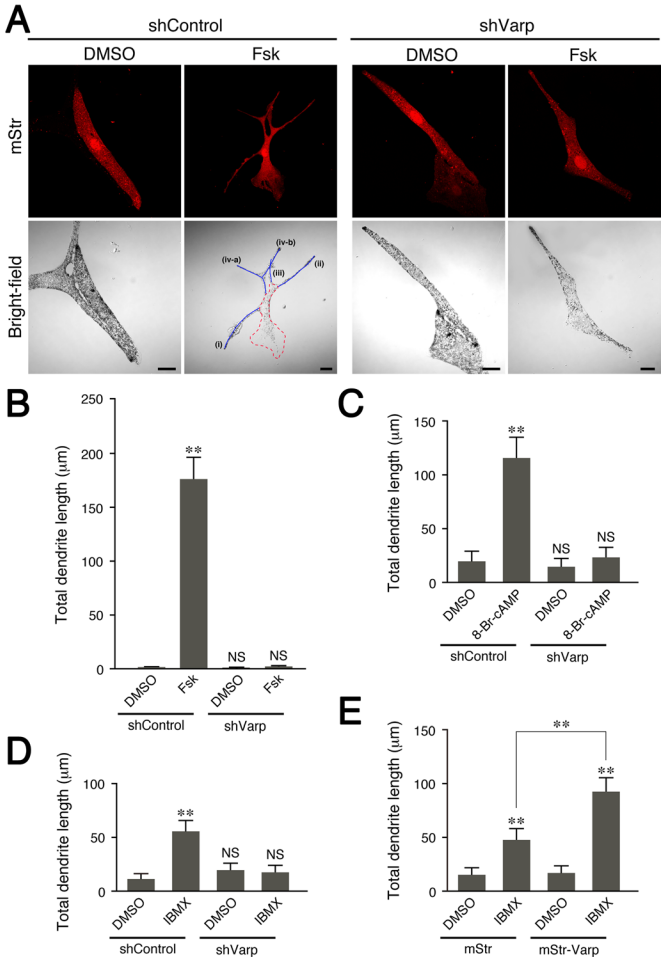

FIGURE 1: Varp is required for forskolin-induced dendrite formation in melanocytes. (A) Melan-a cells were transfected with pmStr-C1 together with pSilencer-Varp (right half) or a control pSilencer vector (left half) and then stimulated for 20 h with 20 μM forskolin (Fsk) or DMSO alone. Images of mStr-expressing cells (i.e., shControl-expressing or shVarp-expressing cells) were captured at random, and typical images of mStr-expressing cells (top) and corresponding bright-field images (bottom) are shown. The total length of their dendrites was measured as described in *Materials and Methods*. For example, the control forskolin-treated cell extended four dendrites (labeled i–iv; dendrite iv has one branch point and two branches, designated vi-a and vi-b, respectively), and length of each dendrite (blue lines) from the edge of the cell body (red, dotted line) to its tip was measured. Scale bars, 20 μm. (B–D) The total dendrite length values (means and SE) of the shVarp-expressing cells and control cells in the presence of forskolin (B), 8-bromo cAMP (8-Br-cAMP) (C), IBMX (D), or DMSO are shown. Note that melan-a cells extended dendrites only in the presence of cAMP-elevating reagents and that such dendrite formation was completely suppressed by the knockdown of endogenous Varp molecules. **$p < 0.01$, in comparison with the control cells (Student's unpaired *t* test). NS, not significant in comparison with the control cells (DMSO + shControl). (E) Effect of overexpression of Varp in melan-a cells on IBMX-induced dendrite formation. Note that expression of Varp in melan-a cells promoted IBMX-induced dendrite formation (but see also Supplemental Figure S1, A and B; expression of Varp did not promote forskolin-induced dendrite formation). **$p < 0.01$, Student's unpaired *t* test.

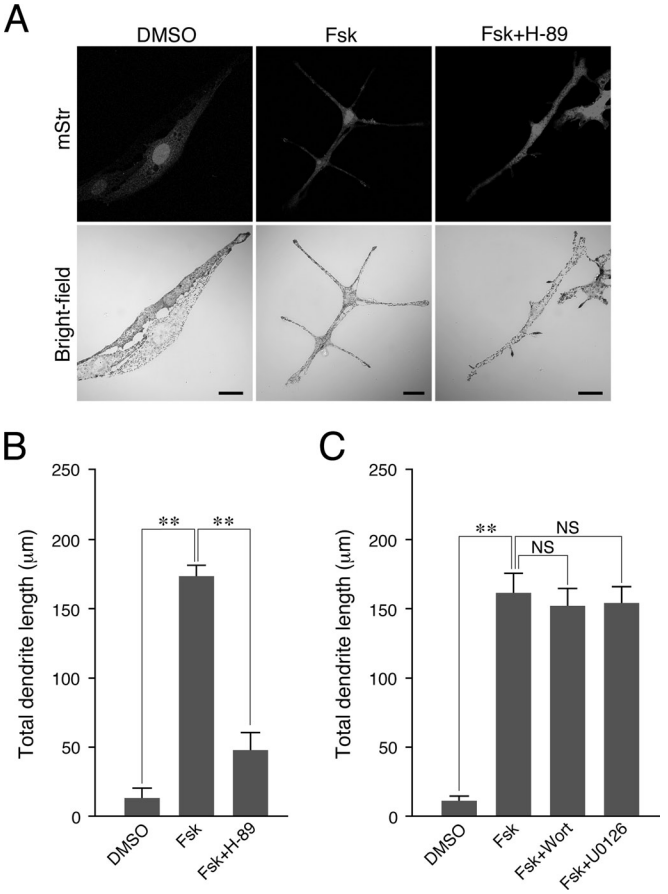

FIGURE 2: Effect of protein kinase inhibitors on forskolin-induced dendrite formation in melan-a cells. (A) Melan-a cells expressing mStr were stimulated for 20 h with 20 μM forskolin (Fsk), 20 μM Fsk + H-89, or DMSO alone. Images of mStr-expressing cells were captured at random, and typical images of mStr-expressing cells (top) and corresponding bright-field images (bottom) are shown. Scale bars, 20 μm. (B) The total dendrite length values (means and SE) of the mStr-expressing cells in the presence of forskolin and H-89 (a PKA inhibitor) are shown. Note that H-89 strongly suppressed forskolin-induced dendrite formation in melan-a cells. **$p < 0.01$, Student's unpaired *t* test. (C) The total dendrite length values (means and SE) of the mStr-expressing cells in the presence of 20 μM forskolin and 100 nM wortmannin (Wort; a PI3-kinase inhibitor) or 20 μM forskolin and 1 μM U0126 (a MEK inhibitor) are shown. Melan-a cells were first treated with wortmannin or U0126 for 6 h in serum-free medium and treated with forskolin (final concentration 20 μM) for 20 h in serum-containing medium that also contained 100 nM wortmannin or 1 μM U0126. Although neither wortmannin nor U0126 inhibited forskolin-induced dendrite formation in the melan-a cells, wortmannin and U0126 clearly inhibited forskolin-induced phosphorylation of Akt and ERK, respectively, under the same experimental conditions (data not shown). **$p < 0.01$, in comparison with the control cells (Student's unpaired *t* test). NS, not significant in comparison with the forskolin-treated cells (Fsk).

contrast to our previous finding that both VPS9 mutants fully support Tyrp1 transport to melanosomes in Varp-deficient melanocytes (Tamura *et al.*, 2011).

We reasoned that if the Rab21-GEF activity of Varp is actually essential for dendrite outgrowth, knockdown of Rab21 should result in a phenotype similar to that of the Varp-deficient melanocytes (i.e., a bipolar phenotype even in the presence of forskolin), and, as expected, knockdown of endogenous Rab21 molecules in melanocytes completely suppressed forskolin-induced dendrite formation (Figure 5A, middle). This inhibition could not be attributable to an off-target effect of the *Rab21* short hairpin RNA (shRNA), because

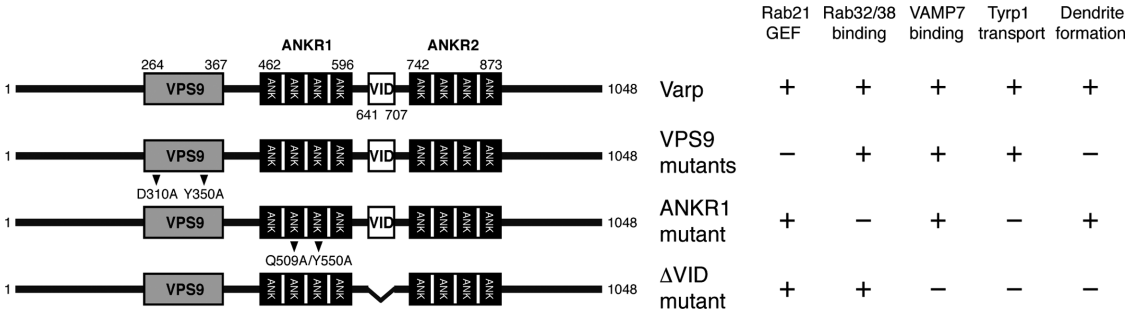

FIGURE 3: Schematic representation of Varp and the Varp mutants used in this study. Varp contains an N-terminal VPS9 domain (i.e., Rab21-GEF domain) and two ankyrin repeats—ANKR1 (i.e., Rab32/38 effector domain) and ANKR2—which are separated by a VID (VAMP7-interaction domain). The Rab21-GEF activity, Rab32/38–binding activity, VAMP7-binding activity, Tyrp1 transport activity, and dendrite formation activity of the wild-type and mutant Varp molecules are summarized at the right of each construct (+ or –). A detailed description of the two VPS9 mutants (D310A and Y350A), ANKR1 mutant (Q509A/Y550A), and ΔVID mutant lacking amino acid residues 641–707 is provided in Tamura *et al.* (2011).

reexpression of enhanced green fluorescent protein (EGFP)–tagged Rab21^{SR} (Supplemental Figure S2) in Rab21-deficient melanocytes clearly restored forskolin-induced dendrite formation (Figure 5, A, right, and B). Moreover, the results of active Rab21 pull-down assays performed with the Rab21-binding domain of APPL1 (Zhu *et al.*, 2007) from melanocyte lysates indicated that Rab21 actually becomes activated 60 min after forskolin treatment (Supplemental Figure S3). These results allowed us to conclude that activation of Rab21 by the Varp VPS9 domain is required for forskolin-induced dendrite formation in melanocytes. Of interest, however, expression of a constitutive-active mutant Rab21(Q76L) or a constitutive-negative mutant Rab21(T31N) in normal melan-a cells had no effect on forskolin-induced dendrite formation (Supplemental Figure S4). Although we do not know the exact reason for their lack of effect, the level of expression of Rab21(Q76L)/(T31N) in melanocytes may be insufficient to function as a dominant-active/negative construct in comparison with the level of endogenous Rab21 protein. To investigate this possibility, siRNA-resistant forms of these Rab21 mutant proteins were expressed in Rab21-deficient cells. As shown in Figure 5C, reexpression of wild-type Rab21^{SR} and Rab21^{SR}(Q76L) clearly restored forskolin-induced dendrite formation, and the total dendrite length of the Rab21^{SR}(Q76L)-reexpressing cells appeared to be longer than that of the Rab21^{SR}-reexpressing cells, although the difference was not statistically significant under our experimental conditions. By contrast, reexpression of Rab21^{SR}(T31N) in Rab21-deficient cells did not restore forskolin-induced dendrite formation. To further highlight the difference between wild-type Rab21 and its constitutive-active mutant (Q76L), we investigated their effect on forskolin-induced dendrite formation in "Varp^{SR}(D310A)-reexpressing Varp-deficient melan-a cells" (Rab21 should not be activated by Varp molecules under these conditions). As expected, only Rab21(Q76L) significantly promoted forskolin-induced dendrite formation (Figure 5D), and the wild-type Rab21 did not promote it, strongly indicating that activation of Rab21 by Varp is necessary for dendrite formation.

The Rab32/38 effector function of Varp is not required for dendrite formation in melanocytes

Next we reexpressed the ANKR1 mutant of Varp^{SR}(Q509A/Y550A) in Varp-deficient melanocytes (Figure 6) to determine the functional involvement of the Rab32/38–binding activity of the ANKR1 domain of Varp in dendrite formation. Although the Varp^{SR}(Q509A/Y550A) mutant completely lacks Rab32/38–binding activity (Tamura *et al.*, 2011), it clearly restored forskolin-induced dendrite formation, the same as the wild-type Varp did (Figure 6, A, middle and bottom, and B). This result was quite unexpected, because we recently showed that neither the Varp^{SR}(Q509A) nor the Varp^{SR}(Y550A) mutant is able to support Tyrp1 transport to melanosomes in melanocytes (Tamura *et al.*, 2011; see also Figure 6C, bottom, second from the right; Tyrp1 signals were almost absent in Varp^{SR}(Q509A/Y550A)-expressing cells). Because the Rab32/38 effector function of Varp is highly unlikely to be required for forskolin-induced dendrite formation in melanocytes, we hypothesized that Rab32 and Rab38 themselves (i.e., ligands of Varp) are also unnecessary for this process. To test our hypothesis, we investigated the dendrite forming ability of Rab32/38–deficient melanocytes, that is, Rab32-knockdown melan-cht cells, which are genetically deficient in *rab38* (Loftus *et al.*, 2002; Wasmeier *et al.*, 2006). As shown in Figure 7, A and B, melan-cht cells were able to form several dendrites in response to forskolin (bottom and next to bottom), despite the Rab32 knockdown. By contrast, knockdown of Varp in melan-cht cells was sufficient to inhibit forskolin-induced dendrite formation (Figure 7, C and D), the same as knockdown of Varp in melan-a cells was. It should be noted, however, that Tyrp1 signals were clearly diminished and clustered around the perinucleus in Rab32/38–deficient melan-cht cells under the same experimental conditions (Supplemental Figure S5, bottom), consistent with previous reports (Wasmeier *et al.*, 2006; Tamura *et al.*, 2011).

VAMP7-binding activity of Varp is required for dendrite formation in melanocytes

We then investigated whether the VAMP7-binding activity of Varp is involved in the forskolin-induced dendrite formation in melanocytes by reexpressing Varp^{SR}-ΔVID in Varp-deficient melanocytes. The results clearly showed that the Varp^{SR}-ΔVID mutant did not restore forskolin-induced dendrite formation in Varp-deficient melanocytes (Figure 8, A and B). In addition, knockdown of endogenous VAMP7 molecules in melanocytes caused complete suppression of forskolin-induced dendrite formation, and reexpression of VAMP7^{SR} in VAMP7-deficient cells restored dendrite formation (Figure 8, C and D). We therefore concluded that the interaction between Varp and VAMP7 is a process that is essential to dendrite outgrowth in melanocytes.

Rab21 and Rab32/38 are present in distinct membrane compartments in melanocytes

The results of the knockdown-rescue experiments described here clearly indicated that activation of Rab21 by Varp is required for

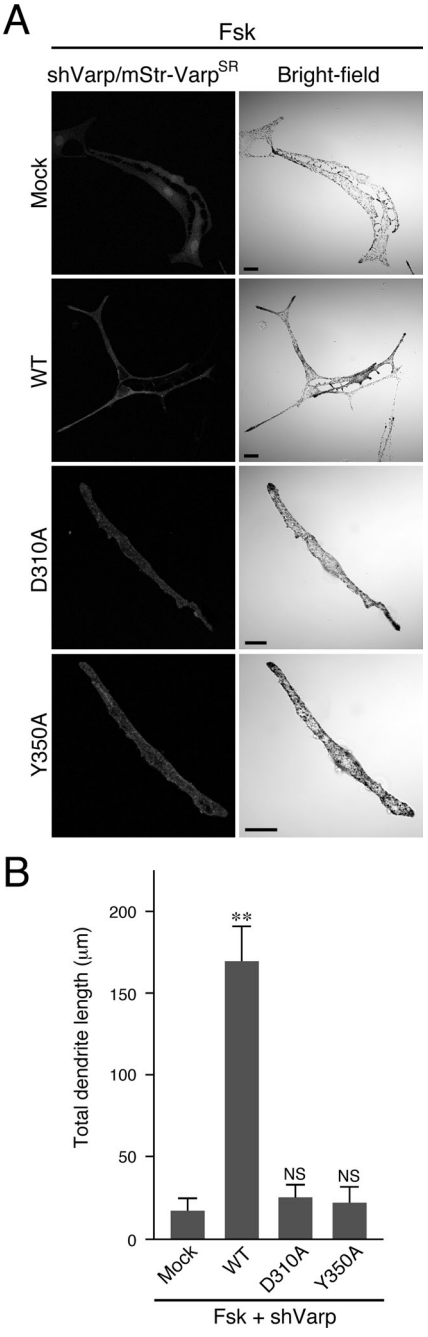

FIGURE 4: Rab21-GEF activity is required for forskolin-induced dendrite formation in melanocytes. (A) Reexpression of Varp^{SR} VPS9 point mutants (D310A and Y350A) in Varp-deficient melan-a cells did not restore dendrite formation. Melan-a cells were transfected with pmStr-C1 (top row), pmStr-C1-Varp^{SR} (second row from the top), pmStr-C1-Varp^{SR}(D310A) (third row from the top), or pmStr-C1-Varp^{SR}(Y350A) (bottom row), together with pSilencer-Varp, and then stimulated with 20 μM forskolin (Fsk) for 20 h. Images of mStr-expressing cells (i.e., shVarp-expressing cells) were captured at random, and the total length of their dendrites was measured as described in *Materials and Methods*. Typical images of mStr-expressing cells (left) and corresponding bright-field images (right) are shown. Scale bars, 20 μm. (B) The total dendrite length values (means and SE) of shVarp/mStr-expressing cells and control cells are shown. Note that neither VPS9 mutant supported forskolin-induced dendrite formation in melanocytes. **p < 0.01, in comparison with the control cells (Student's unpaired *t* test). NS, not significant in comparison with the mock control cells.

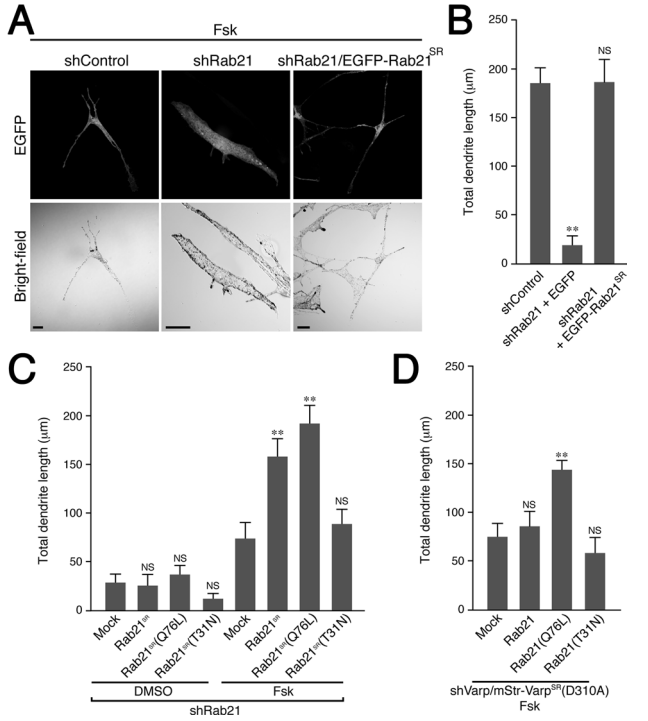

FIGURE 5: Rab21 is required for forskolin-induced dendrite formation in melanocytes. (A) Effect of knockdown of endogenous Rab21 molecules on forskolin-induced dendrite formation in melan-a cells. Melan-a cells were cotransfected with pEGFP-C1 and a control pSilencer vector (left), pEGFP-C1and pSilencer-Rab21 (middle), or EGFP-C1-Rab21^{SR} and pSilencer-Rab21 (right) and then stimulated with 20 μM forskolin (Fsk) for 20 h. Images of EGFP-expressing cells were captured at random, and the total length of their dendrites was measured as described in *Materials and Methods*. Typical images of pEGFP-expressing cells (top) and corresponding bright-field images (bottom) are shown. Scale bars, 20 μm. (B) The total dendrite length values (means and SE) of shControl/EGFP–expressing, shRab21/EGFP–expressing, and shRab21/EGFP-Rab21^{SR}–expressing cells are shown. Note that knockdown of endogenous Rab21 molecules completely inhibited forskolin-induced dendrite formation in melanocytes and that reexpression of EGFP-Rab21^{SR} in Rab21-deficient melan-a cells completely restored forskolin-induced dendrite formation. **p < 0.01, in comparison with the control cells (Student's unpaired *t* test). NS, not significant in comparison with the control cells. (C) The total dendrite length values (means and SE) of EGFP-Rab21^{SR}–reexpressing, EGFP-Rab21^{SR}(Q76L)–reexpressing, and EGFP-Rab21^{SR}(T31N)–reexpressing Rab21-deficient cells are shown. Melan-a cells were cotransfected with pSilencer-Rab21 and pEGFP-C1-Rab21^{SR}, pSilencer-Rab21 and pEGFP-C1-Rab21^{SR}(Q76L), or pSilencer-Rab21 and pEGFP-C1-Rab21^{SR}(T31N) and then stimulated with 20 μM forskolin for 20 h. Note that reexpression of Rab21^{SR} or Rab21^{SR}(Q76L), but not of Rab21^{SR}(T31N), restored forskolin-induced dendrite formation in Rab21-deficient melan-a cells (but see Supplemental Figure S4B; expression of Rab21 or Rab21(Q76L) in normal melan-a cells had no effect on forskolin-induced dendrite formation). (D) The total dendrite length values (means and SE) of EGFP-Rab21/mStr-Varp^{SR}(D310A)–expressing, EGFP-Rab21(Q76L)/mStr-Varp^{SR}(D310A)–expressing, and EGFP-Rab21(T31N)/mStr-Varp^{SR}(D310A)–expressing Varp-deficient cells are shown. Melan-a cells were cotransfected with pEGFP-C1-Rab21 (wild type, Q76L, or T31N), or pEGFP-C1 alone, and pmStr-C1-Varp^{SR}(D310A) together with pSilencer-Varp and then stimulated with 20 μM forskolin for 20 h. Note that expression of Rab21(Q76L), but not of the wild-type protein, in Varp^{SR}(D310A)–reexpressing cells promoted forskolin-induced dendrite formation. **p < 0.01 (Student's unpaired *t* test); NS, not significant in comparison with the mock control cells.

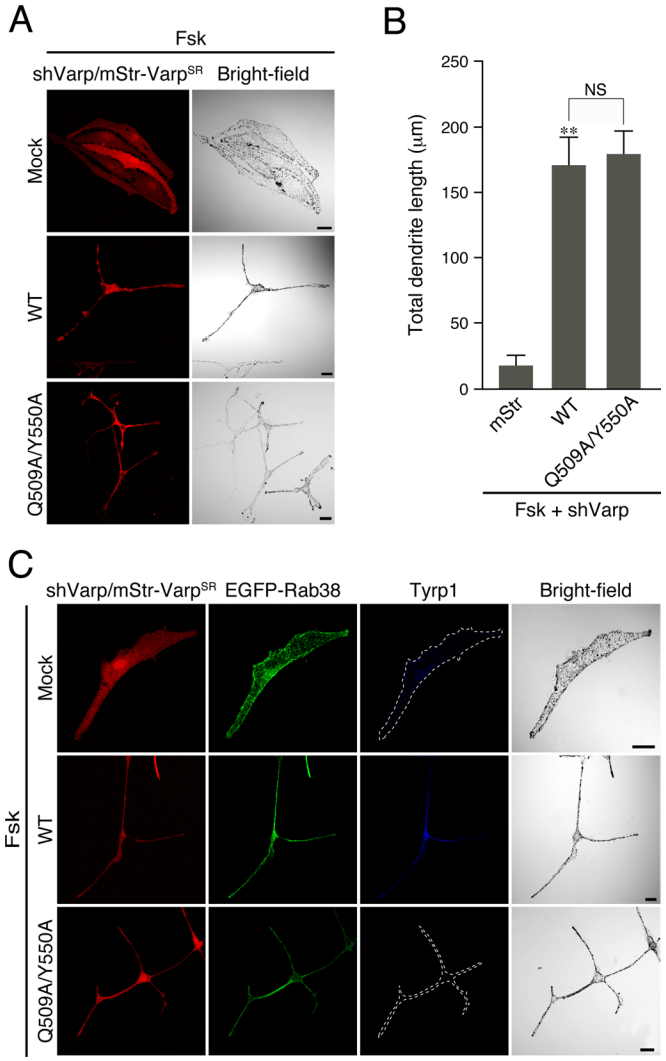

FIGURE 6: Rab32/38–binding activity is not required for forskolin-induced dendrite formation in melanocytes. (A) Reexpression of a Varp^{SR} ANKR1 point mutant (Q509A/Y550A) in Varp-deficient melan-a cells completely restored dendrite formation. Melan-a cells were transfected with pmStr-C1 (top), pmStr-C1-Varp^{SR} (middle), or pmStr-C1-Varp^{SR}(Q509A/Y550A) (bottom) together with pSilencer-Varp and then stimulated with 20 μM forskolin (Fsk) for 20 h. Images of mStr-expressing cells (i.e., shVarp-expressing cells) were captured at random, and the total length of their dendrites was measured as described in *Materials and Methods*. Typical images of mStr-expressing cells (left) and corresponding bright-field images (right) are shown. Scale bars, 20 μm. (B) The total dendrite length values (means and SE) of shVarp/mStr-Varp^{SR}–expressing cells and control shVarp/mStr–expressing cells are shown. Note that the ANKR1 point mutant (Q509A/Y550A), which completely lacks Rab32/38–binding activity (Tamura *et al.*, 2011), completely restored forskolin-induced dendrite formation in Varp-deficient melanocytes. **$p < 0.01$, in comparison with the control cells (Student's unpaired *t* test). NS, not significant in comparison with the wild-type Varp-expressing cells. (C) The Varp(Q509A/Y550A) mutant did not rescue Tyrp1 deficiency in Varp-deficient melan-a cells but did restore forskolin-induced dendrite formation. Melan-a cells were cotransfected with pmStr-C1 and pEGFP-C1-Rab38 (top), pmStr-C1-Varp^{SR} and pEGFP-C1-Rab38 (middle), or pmStr-C1-Varp^{SR}(Q509A/Y550A) and pEGFP-C1-Rab38 (bottom) together with pSilencer-Varp (Tamura *et al.*, 2011) and then stimulated with 20 μM forskolin (Fsk) for 20 h. The cells were immunostained with anti-Tyrp1 mouse monoclonal antibody (blue, middle right). Typical images of mStr-expressing cells (red) and EGFP-Rab38-expressing cells (green) (far left and second column from the left, respectively) and corresponding bright-field images (far right) are shown. Note the clearly reduced Tyrp1 signals in the Varp-deficient cell and the Varp^{SR}(Q509A/Y550A)–reexpressing cell (the cells are outlined in white). Scale bars, 20 μm.

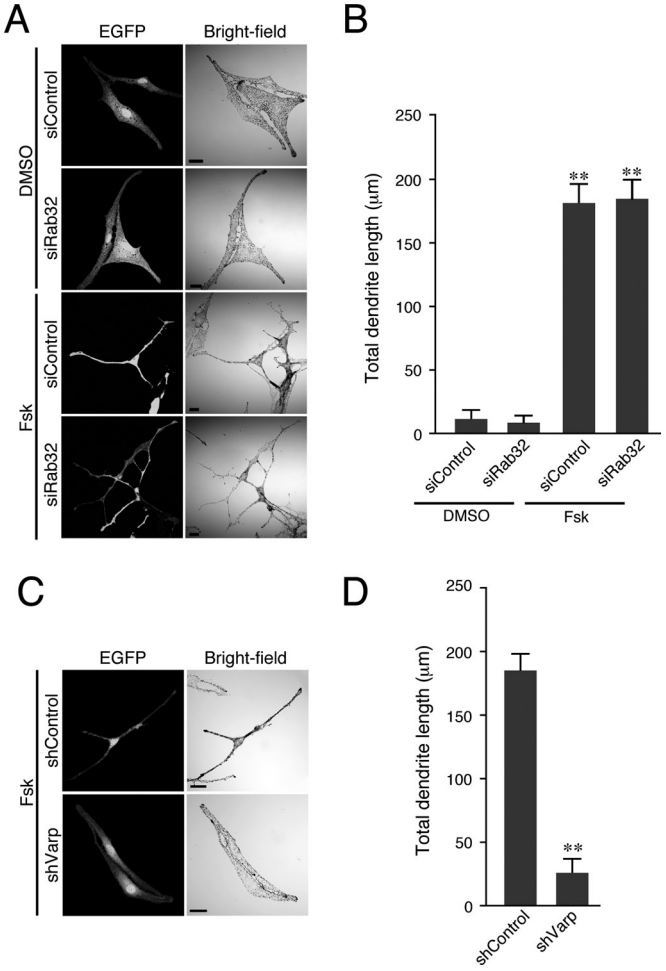

FIGURE 7: Rab32/38 are not required for forskolin-induced dendrite formation in melanocytes. (A) Effect of knockdown of endogenous Rab32 molecules on forskolin-induced dendrite formation in melan-cht cells (i.e., Rab32/38–deficient cells). Melan-cht cells were cotransfected with pEGFP-C1 and a control siRNA (top and third row) and with pEGFP-C1 and siRab32 (second and bottom row) and then stimulated for 20 h with 20 μM forskolin (Fsk; third and bottom row) or DMSO alone (top and second row). Images of EGFP-expressing cells (i.e., siControl-expressing or siRab32-expressing cells) were captured at random, and the total length of their dendrites was measured as described in *Materials and Methods*. Typical images of EGFP-expressing cells (left) and corresponding bright-field images (right) are shown. Scale bars, 20 μm. (B) The total dendrite length values (means and SE) of siControl/EGFP–expressing and siRab32/EGFP–expressing cells are shown. Note that knockdown of endogenous Rab32 molecules had no effect on dendrite formation in Rab38-deficient melan-cht cells. **$p < 0.01$, in comparison with the control cells (siControl + DMSO; Student's unpaired *t* test). (C) Effect of knockdown of Varp in Rab32/38–deficient melan-cht cells on forskolin-induced dendrite formation. Melan-cht cells were transfected with pEGFP-C1 together with pSilencer-Varp (bottom) or a control pSilencer vector (top) and then stimulated with 20 μM forskolin (Fsk) for 20 h. Typical images of EGFP-expressing cells (left) and corresponding bright-field images (right) are shown. Scale bars, 20 μm. (D) The total dendrite length values (means and SE) of shVarp-expressing cells and control cells are shown. **$p < 0.01$, in comparison with the control cells (Student's unpaired *t* test).

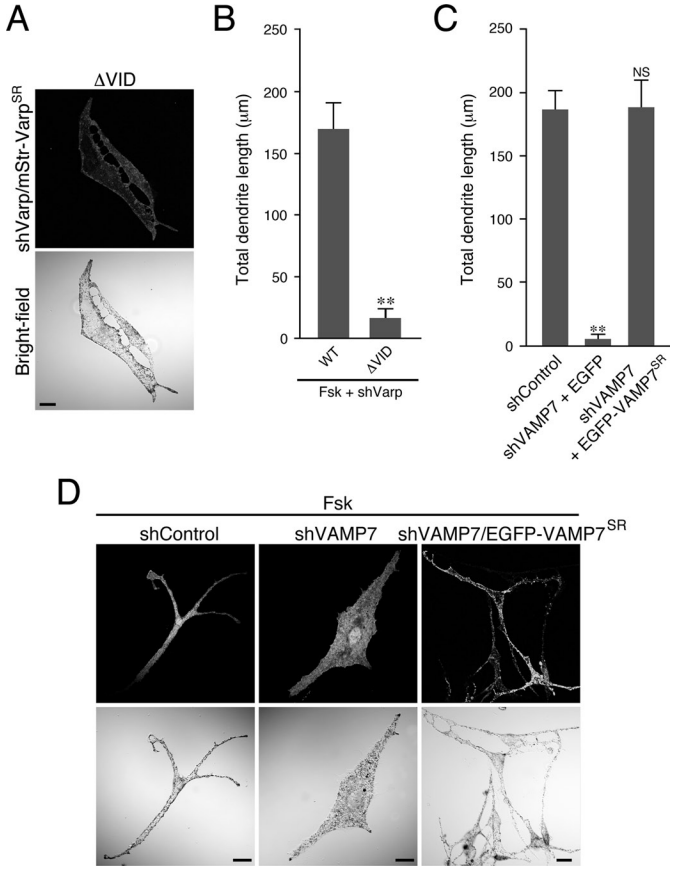

FIGURE 8: VAMP7-binding activity of Varp and VAMP7 is required for forskolin-induced dendrite formation in melanocytes. (A) Reexpression of a Varp^{SR}-ΔVID mutant in Varp-deficient melan-a cells did not restore dendrite formation. Melan-a cells were transfected with pmStr-C1-Varp^{SR}-ΔVID together with pSilencer-Varp and then stimulated with 20 μM forskolin (Fsk) for 20 h. Images of mStr-Varp^{SR}-ΔVID–expressing cells were captured at random, and the total length of their dendrites was measured as described in *Materials and Methods*. Typical images of mStr-Varp^{SR}-ΔVID–expressing cells (top) and corresponding bright-field images (bottom) are shown. Scale bar, 20 μm. (B) The total dendrite length values (means and SE) of shVarp/mStr-Varp–expressing and mStr-Varp^{SR}-ΔVID–expressing cells are shown. Note that the ΔVID mutant did not support forskolin-induced dendrite formation in melanocytes. **$p < 0.01$, in comparison with the control wild-type Varp-expressing cells (Student's unpaired *t* test). (C) The total dendrite length values (means and SE) of shControl/EGFP–expressing, shVAMP7/EGFP–expressing, and shVAMP7/EGFP-VAMP7^{SR}–expressing cells are shown. **$p < 0.01$, in comparison with the control cells (Student's unpaired *t* test). NS, not significant in comparison with the control cells. (D) Effect of knockdown of endogenous VAMP7 molecules on forskolin-induced dendrite formation in melan-a cells. Melan-a cells were cotransfected with pEGFP-C1 and a control pSilencer vector (left), pEGFP-C1 and pSilencer-VAMP7 (middle), or pEGFP-C1-VAMP7^{SR} and pSilencer-VAMP7 (right) and then stimulated with 20 μM forskolin (Fsk) for 20 h. Images of EGFP-expressing cells were captured at random, and the total length of their dendrites was measured as described in *Materials and Methods*. Typical images of EGFP-expressing cells (top) and corresponding bright-field images (bottom) are shown. Scale bars, 20 μm. Note that knockdown of endogenous VAMP7 molecules completely inhibited forskolin-induced dendrite formation in melanocytes, whereas reexpression of EGFP-VAMP7^{SR} in VAMP7-deficient melan-a cells completely restored forskolin-induced dendrite formation.

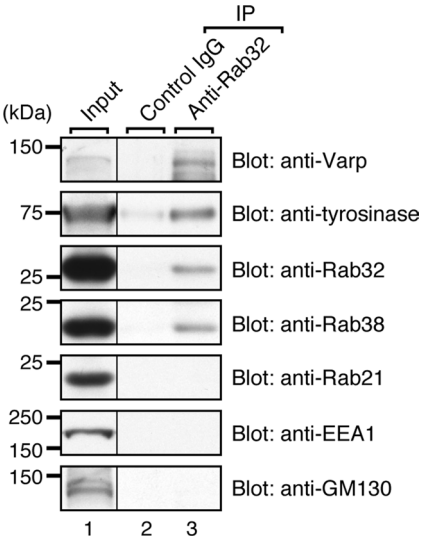

FIGURE 9: Rab21 and Rab32/38 are present in distinct membrane compartments in melanocytes. Immunoaffinity purification of Rab32-containing vesicles/organelles from crude membrane fractions of B16-F1 cells was performed by using anti-Rab32 IgG (lane 3) or control rabbit IgG (lane 2) as described in *Materials and Methods*. The Rab32-containing membrane compartment was analyzed by 10% SDS–PAGE, followed by immunoblotting with anti-Varp antibody (0.4 μg/ml), anti-tyrosinase antibody (0.3 μg/ml), anti-Rab32 antibody (1.5 μg/ml), anti-Rab38 antibody (0.9 μg/ml), anti-Rab21 antibody (0.2 μg/ml), anti-EEA1 antibody (1/1000 dilution), and anti-GM130 antibody (0.3 μg/ml). Note that Rab21 was not copurified with the Rab32-membrane compartment, which clearly includes Rab38, tyrosinase, and Varp but not EEA1 or GM130. Input means 1% volume of the crude membrane fractions used for immunoaffinity purification. The positions of the molecular mass markers (in kilodaltons) are shown on the left.

forskolin-induced dendrite formation in melanocytes and that the Rab32/38 effector function of Varp is not. We therefore hypothesized that Varp regulates dendrite outgrowth via a pathway that is independent of Rab32/38–mediated membrane trafficking—in other words, that the Rab32/38–containing membrane compartment and Rab21-containing membrane compartment are different. To test our hypothesis, we finally attempted to determine whether Rab21 is present in the Rab32/38–containing membrane compartment biochemically by performing a vesicle/organelle pull-down assay with specific antibodies. As expected, the Rab32-containing membrane compartment purified by the anti–Rab32-specific antibody did not contain either Rab21 or EEA1 (an early endosome marker), but it clearly contained Rab38 (which redundantly regulates trafficking of melanogenic enzymes, tyrosinase and Tyrp1, together with Rab32; Wasmeier *et al.*, 2006), tyrosinase (a cargo of Rab32/38–containing vesicles/organelles; Wasmeier *et al.*, 2006), and Varp (Rab32-binding protein; Tamura *et al.*, 2009; Figure 9). We also tried the reverse approach, but, unfortunately, the anti-Rab21 antibody we used was inappropriate for a vesicle/organelle pull-down assay (data not shown). To overcome this problem, we compared the subcellular localization of HA-Rab21 and FLAG-Rab32/38 by means of an immunofluorescence analysis of melan-a cells, and consistent with the results of the vesicle/organelle pull-down assay, no colocalization between HA-Rab21 and FLAG-Rab32/38 was observed (Supplemental Figure S6).

DISCUSSION

We previously showed that Varp together with Rab32/38 regulates Tyrp1 trafficking to melanosomes in melanocytes and that activation of Rab21 by Varp (or Rab21 itself) is not needed for this process to occur (Tamura *et al.*, 2009, 2011). In the present study, we discovered a novel function of Varp in melanocytes, that is, regulation of forskolin-stimulated dendrite formation (Figure 1), a function that is believed to be required for efficient melanosome transfer from melanocytes to neighboring keratinocytes. However, the results we obtained were the opposite of the results obtained when we investigated the role of Varp in Tyrp1 trafficking to melanosomes. Both the Rab21-GEF activity of Varp and its substrate Rab21 are required for forskolin-induced dendrite formation (Figures 4 and 5), whereas the Rab32/38–binding activity of Varp and its ligand Rab32/38 are not (Figures 6 and 7). Furthermore, Rab21-containing vesicles and Rab32/38–containing vesicles are distributed differently in melanocytes (Figure 9 and Supplemental Figure S6). We therefore concluded that Varp regulates two independent membrane trafficking pathways in the same melanocyte—that is, the membrane-trafficking pathway involved in dendrite formation and the membrane-trafficking pathway involved in Tyrp1 trafficking to melanosomes—via two distinct domains—its VPS9/Rab21-GEF domain and its ANKR1/Rab32/38 effector domain, respectively—although the VID domain (and its ligand VAMP7) is required for both pathways (Figure 8; Tamura *et al.*, 2011). Possible mechanisms by which Varp regulates two distinct membrane trafficking pathways are illustrated in Supplemental Figure S7.

How does Rab21 promote dendrite formation in melanocytes? We believe that dendrite formation in melanocytes requires the occurrence of at least two different processes: cytoskeletal rearrangement (e.g., reorganization of the actin cytoskeleton) and supply of new membranes/proteins to elongate dendrites (e.g., transport of endosome-derived vesicles to the tip of dendrites, as proposed for the role of endosomal trafficking in neurite outgrowth in neurons; reviewed in Sann *et al.*, 2009). Because Rab21 (and also VAMP7) is a membrane-trafficking protein and has been shown to be involved in endosomal trafficking (Simpson *et al.*, 2004; Pellinen *et al.*, 2006; Zhang *et al.*, 2006; Chaineau *et al.*, 2009), Rab21 is likely to be involved in the process of supplying new membranes/proteins to elongate dendrites rather than in the process of cytoskeletal rearrangement. Furthermore, since overexpression of Rab21(Q76L) alone (i.e., activation of Rab21) was unable to induce dendrite formation in melanocytes (Figure 5C), additional factors, for example, other types of small GTPases, that induce cytoskeletal rearrangement are also required for dendrite formation in melanocytes. Actually, our preliminary data showed that overexpression of a dominant-negative form of Rac1 strongly inhibited forskolin-induced dendrite formation in melan-a cells (A. Yatsu, N. Ohbayashi, and M. Fukuda, unpublished data). We therefore speculate that forskolin (presumably PKA) activates both Rab21-dependent endosomal trafficking, which contributes to membrane addition for dendrite outgrowth, and cytoskeletal rearrangement, which is presumably mediated by other types of small GTPases (e.g., Rac1). Further extensive research will be necessary to elucidate the precise downstream mechanism of Rab21 and the mechanism that regulates cytoskeletal rearrangement during dendrite formation in melanocytes.

Thus far, several Rab-GEFs, including Sec2p and Rabin8, have been shown to bind a nonsubstrate Rab protein via a domain other than a GEF domain (Ortiz *et al.*, 2002; Knödler *et al.*, 2010). These Rab GEFs have been reported to play bifunctional roles, that is, a Rab-GEF role and a Rab effector role, in the "same" membrane-trafficking pathway by sequential mechanisms (i.e., a Rab GEF cascade; Stenmark, 2009; Hutagalung and Novick, 2011). As an example, Ypt31/32p recruits Sec2p to secretory vesicles, and then Sec2p activates Sec4p on secretory vesicles in budding yeasts (Ortiz *et al.*, 2002). Rabin8, a mammalian Sec2 homologue that acts as a Rab8-GEF (Hattula *et al.*, 2002), also functions as a Rab11A effector during epithelial polarization (Bryant *et al.*, 2010). It should be noted that Rab11 binding to Rabin8 promotes Rab8-GEF activity in vitro (Knödler *et al.*, 2010). Our finding that the Rab21-GEF activity of the VPS9 domain and the Rab32/38–binding activity of the ANKR1 domain of Varp function independently in melanocytes is in sharp contrast to the previous finding about other Rab-binding GEFs. To our knowledge, this study is the first to demonstrate that two distinct Rab signaling domains of Varp (i.e., the Rab21-GEF domain and the Rab32/38 effector domain) independently regulate different membrane-trafficking pathways within a single cell, although we cannot completely rule out the possibility that Rab21-GEF Varp constitutes a Rab-GEF cascade together with an unidentified Rab other than Rab32/38 during dendrite formation in melanocytes.

What is the regulatory mechanism of the activation of Rab21 by Varp and the Rab32/38 effector function of Varp in melanocytes? These are open questions, but we believe that the Rab21-GEF activity and Rab32/38–binding activity of Varp are independently regulated in melanocytes, because the VPS9 point mutants and Rab32/38-binding–deficient mutant of Varp were found to be fully capable of mediating the Tyrp1 trafficking to melanosomes and forskolin-induced dendrite formation, respectively, in Varp-deficient melanocytes (Tamura *et al.*, 2011 and this study). Because the Rab21-GEF activity of Varp is required for staurosporine-induced neurite outgrowth in PC12 cells (Burgo *et al.*, 2009) and forskolin-induced dendrite formation in melan-a cells (this study), and both staurosporine and forskolin may modulate protein kinase (e.g., PKC and PKA) cascades, phosphorylation of Varp might be involved in regulation of the Rab21-GEF activity of Varp. Actually, the forskolin-induced dendrite formation was clearly suppressed by the PKA inhibitor H-89 (Figure 2, A and B), indicating that PKA is involved in this process. Further work will be necessary to determine the mechanism by which PKA stimulates the Rab21-GEF activity at the molecular level.

In conclusion, the results of the knockdown-rescue experiments in this study showed that activation of Rab21 by the Varp VPS9 domain is required for forskolin-induced dendrite formation and that the Rab32/38 effector function of Varp is not. By contrast, the Rab32/38 effector function of Varp, but not its Rab21-GEF activity, has been shown to be required for Tyrp1 trafficking to melanosomes (Tamura *et al.*, 2011). Because these findings indicated the presence of a novel mechanism in which two Rab signaling domains in a single Varp molecule, that is, the Rab21-GEF domain and the Rab32/38 effector domain, regulate different membrane-trafficking pathways, that is, dendrite formation and Tyrp1 transport, respectively, Varp contributes to efficient skin darkening by coupling these two distinct processes. Because Varp is expressed in a variety of mouse tissues and cell lines (Zhang *et al.*, 2006), it would be interesting to determine whether the function of the two domains of Varp is also regulated independently in other cells besides melanocytes.

MATERIALS AND METHODS

Materials

Anti-Tyrp1 mouse monoclonal antibody (Ta99) was obtained from ID Labs (London, Canada). Anti-actin goat polyclonal antibody and anti-actin mouse monoclonal antibody were from Santa Cruz Biotechnology (Santa Cruz, CA) and Applied Biological Materials (Richmond, Canada), respectively. Anti-EEA1 mouse monoclonal

antibody and anti-GM130 mouse monoclonal antibody were from Cell Signaling Technology (Danvers, MA) and BD Biosciences (San Jose, CA), respectively. Anti-FLAG tag rabbit polyclonal antibody and anti-HA tag mouse monoclonal antibody were from Sigma-Aldrich (St. Louis, MO) and Roche Molecular Biochemicals (Mannheim, Germany), respectively. Anti-GFP (green fluorescent protein) rabbit polyclonal antibody, horseradish peroxidase (HRP)-conjugated anti-GFP antibody, and HRP-conjugated red fluorescent protein antibody were from MBL (Nagoya, Japan). HRP-conjugated anti–glutathione *S*-transferase (GST) antibody was from Santa Cruz Biotechnology. Alexa 488/594–conjugated anti–mouse immunoglobulin (IgG) goat antibody was from Invitrogen (Carlsbad, CA). Anti-Varp rabbit polyclonal antibody, anti-Rab21 rabbit polyclonal antibody, anti-Rab32 rabbit polyclonal antibody, and anti-Rab38 rabbit polyclonal antibody were prepared as described previously (Tamura *et al.*, 2009, 2011). Anti-tyrosinase rabbit polyclonal antibody was raised against a peptide corresponding to the C-terminal sequence (amino acid residues 520–533) of mouse tyrosinase (Jiménez *et al.*, 1991; Beaumont *et al.*, 2011) and then affinity-purified essentially as described previously (Fukuda and Mikoshiba, 1999). All other reagents used in this study were analytical grade or the highest grade commercially available.

Plasmid constructions

Mouse monomeric Strawberry (mStr)–tagged Varp expression plasmids carrying a D310A, Y350A, or Q509A/Y550A mutation or carrying a deletion of amino acid residues 641–707 (named ΔVID; Burgo *et al.*, 2009) were prepared as described previously (Tamura *et al.*, 2011). pSilencer-Varp, pSilencer-VAMP7, pSilencer-Rab21, pmStr-C1-Varp^{SR} (siRNA resistant), pEF-FLAG-Rab32/38, pEGFP-C1-Rab21(Q76L), pEGFP-C1-Rab21(T31N), and pEGFP-C1-VAMP7^{SR} were also prepared as described previously (Tamura *et al.*, 2009, 2011). pEF-HA-Rab21 was prepared by subcloning the Rab21 fragment into the pEF-HA expression vector (Fukuda, 2002). The knockdown efficiency of each pSilencer vector and siRNA resistance of Varp^{SR} (or VAMP7^{SR}) have been described elsewhere (Tamura *et al.*, 2009, 2011). cDNA encoding the Rab21-binding site of mouse APPL1 (adaptor protein containing PH domain, PTB domain, and leucine zipper motif; amino acids 5–377; named APPL1-N; Zhu *et al.*, 2007) was amplified by conventional PCR techniques and subcloned into the pEF-T7-GST vector modified from pEF-BOS (Fukuda *et al.*, 1999). All Varp mutant proteins were strongly expressed in the melanocytes, the same as the wild-type protein was (Tamura *et al.*, 2011; Supplemental Figure S1D), and their expression in melan-a cells alone had no effect on forskolin-induced dendrite formation (Supplemental Figure S1C). The siRNA against Rab32 (Oligo 32-1) was synthesized as described previously (Wasmeier *et al.*, 2006). pEGFP-C1-Rab21^{SR}, pEGFP-C1-Rab21^{SR}(Q76L), and pEGFP-C1-Rab21^{SR}(T31N) were produced by using the same method described previously (Tamura *et al.*, 2011) using the following mutagenic oligonucleotides (substituted nucleotides are shown in italics): 5′-CCCAAT*C*TA*T*TA*T*CG*G*GA*C*TC*T*AACGGAGC-3′ (Rab21 SR-5′ primer, sense) and 5′-CCTCCGTTAGA*G*TCCCGATAATA*G*ATT-GGG-3′ (Rab21 SR-3′ primer, antisense). The siRNA resistance of Rab21^{SR} was checked by coexpressing *Rab21* shRNA and pEGFP-Rab21^{SR} in COS-7 cells (Supplemental Figure S2).

Forskolin-induced dendrite formation in melanocytes

The immortal mouse melanocyte cell line melan-a, derived from a black mouse, and melan-cht, derived from a *chocolate* mouse, both generous gifts of Dorothy C. Bennett (St George's Hospital Medical School, London, United Kingdom), were cultured on glass-bottom dishes (35-mm dish; MatTek, Ashland, MA; Bennett *et al.*, 1987; Kuroda *et al.*, 2003). Cotransfection of pmStr-C1-Varp^{SR} and pSilencer-Varp (or control pSilencer alone), pEGFP-C1-VAMP7^{SR} and pSilencer-VAMP7 (or pSilencer), or pEGFP-C1-Rab21^{SR} and pSilencer-Rab21 (or pSilencer) was achieved by using FuGENE 6 (Roche Molecular Biochemicals) according to the manufacturer's instructions. Cells were treated with 20 μM forskolin (Sigma-Aldrich), 10 μM IBMX (Nacalai Tesque, Kyoto, Japan), 100 μM 8-bromo cAMP (Sigma-Aldrich), or DMSO alone (control) 1 d after transfection. Twenty hours after the drug treatment, the cells were fixed in 4% paraformaldehyde and examined for fluorescence with a confocal fluorescence microscope (FluoView; Olympus, Tokyo, Japan). The images of the EGFP-expressing cells (for VAMP7 and Rab21) and mStr-expressing cells (for Varp) were captured at random ($n > 30$ from three independent dishes) with the confocal microscope, and the total length of their dendrites was measured with ImageJ software (version 1.43u; National Institutes of Health, Bethesda, MD). Length of each dendrite was measured from the edge of the cell body to the tip of dendrites, and total dendrite length means the sum of each dendrite length (see Figure 1A, middle left).

Immunofluorescence analysis

Melan-a cells (or melan-cht cells) were cotransfected with pmStr-C1-Varp^{SR} (or pmStr-C1-Varp^{SR}(Q509A/Y550A)) and pSilencer-Varp (or control pSilencer alone) as described. Two days after transfection, the cells were fixed in 4% paraformaldehyde, permeabilized with 0.3% Triton X-100, stained with anti-Tyrp1 mouse monoclonal antibody (1/100 dilution), and then visualized with anti–mouse Alexa Fluor 488 IgG and examined for fluorescence with a confocal fluorescence microscope as described. The images of the cells were processed with Adobe Photoshop software (CS4; San Jose, CA).

Active GTP-Rab21 pull-down assays

GTP-Rab21 pull-down assays were performed essentially as described previously (Itoh and Fukuda, 2006). In brief, pEF-T7-GST, pEF-T7-GST-APPL1-N, pEGFP-Rab21(T31N), or pEGFP-Rab21(Q76L) was transfected into COS-7 cells with Lipofectamine-LTX-PLUS (Invitrogen) according to the manufacturer's instructions. Two days after transfection, the cells were harvested and lysed with a lysis buffer (50 mM 4-(2-hydroxyethyl)-1-piperazineethanesulfonic acid [HEPES]–KOH at pH 7.2, 150 mM NaCl, 1 mM $MgCl_2$, and 1% Triton X-100) containing appropriate protease inhibitors. Glutathione–Sepharose beads (GE Healthcare, Little Chalfont, United Kingdom) coupled with T7-GST-APPL1-N (or T7-GST alone) were incubated for 1 h with the COS-7 cell lysates containing EGFP-Rab21(T31N) and EGFP-Rab21(Q76L) in the presence of 1 mM GDP and 0.5 mM GTPγS, respectively. After washing the beads three times, proteins bound to the beads were subjected to 10% SDS–PAGE, followed by immunoblotting with HRP-conjugated anti-GFP antibody and HRP-conjugated anti-GST antibody. pEF-FLAG-Rab21 was transfected into B16-F1 cells with Lipofectamine-LTX-PLUS. One day after transfection, the cells were treated with 20 μM forskolin for 30–120 min, and they were then harvested and lysed with the lysis buffer as described. Glutathione–Sepharose beads coupled with T7-GST-APPL1-N were incubated for 1 h with the B16-F1 cell lysates without further addition of guanine nucleotides. Active GTP-Rab21 was detected in a manner similar to that described.

Immunoaffinity purification of a Rab32-containing membrane compartment

Immunoaffinity purification of a Rab32-containing membrane compartment with anti-Rab32 IgG–conjugated magnetic beads was

performed essentially as described previously (Kuroda and Fukuda, 2004). In brief, Dynabeads M-280 (30-µl wet volume) coated covalently with sheep anti–rabbit IgG (Invitrogen) was incubated for 3 h at 4°C with the anti-Rab32 antibody or control rabbit IgG (5 µg) in phosphate-buffered saline (PBS) containing 0.1% bovine serum albumin. B16-F1 cells (one confluent 10-cm dish) were homogenized in a homogenization buffer (5 mM HEPES-KOH at pH 7.2, 5 mM ethylene glycol tetraacetic acid, 1 mM $MgCl_2$, 0.03 M sucrose, and appropriate protease inhibitors), and, after centrifugation at 800 × *g* for 10 min, the supernatant was incubated with the primary antibody-coated beads for 1 h at 4°C in the homogenization buffer containing 10% fetal bovine serum. After washing the beads twice with PBS, the bound fractions were analyzed by 10% SDS–PAGE, followed by immunoblotting with anti-EEA1 antibody, anti-GM130 antibody, anti-tyrosinase antibody, anti-Rab21 antibody, anti-Rab32 antibody, anti-Rab38 antibody, and anti-Varp antibody.

ACKNOWLEDGMENTS

We thank Dorothy C. Bennett for kindly donating melan-a and melan-cht cells, Megumi Aizawa for technical assistance, and members of the Fukuda laboratory for valuable discussions. This work was supported in part by Grants-in-Aid for Scientific Research from the Ministry of Education, Culture, Sports, and Technology of Japan (to N.O. and M.F.), by a grant from the Global Center of Excellence Program (Basic and Translational Research Center for Global Brain Science) of the Ministry of Education, Culture, Sports, and Technology of Japan (to N.O. and M.F.), and by a grant from the Kato Memorial Bioscience Foundation (to M.F.).

REFERENCES

Barr F, Lambright DG (2010). Rab GEFs and GAPs. Curr Opin Cell Biol 22, 461–470.

Beaumont KA *et al*. (2011). The recycling endosome protein Rab17 regulates melanocytic filopodia formation and melanosome trafficking. Traffic 12, 627–643.

Bennett DC, Cooper PJ, Hart IR (1987). A line of non-tumorigenic mouse melanocytes, syngeneic with the B16 melanoma and requiring a tumour promoter for growth. Int J Cancer 39, 414–418.

Bryant DM, Datta A, Rodríguez-Fraticelli AE, Peränen J, Martín-Belmonte F, Mostov KE (2010). A molecular network for de novo generation of the apical surface and lumen. Nat Cell Biol 12, 1035–1045.

Burgo A, Sotirakis E, Simmler MC, Verraes A, Chamot C, Simpson JC, Lanzetti L, Proux-Gillardeaux V, Galli T (2009). Role of Varp, a Rab21 exchange factor and TI-VAMP/VAMP7 partner, in neurite growth. EMBO Rep 10, 1117–1124.

Carney DS, Davies BA, Horazdovsky BF (2006). Vps9 domain-containing proteins: activators of Rab5 GTPases from yeast to neurons. Trends Cell Biol 16, 27–35.

Chaineau M, Danglot L, Galli T (2009). Multiple roles of the vesicular-SNARE TI-VAMP in post-Golgi and endosomal trafficking. FEBS Lett 583, 3817–3826.

Delprato A, Lambright DG (2007). Structural basis for Rab GTPase activation by VPS9 domain exchange factors. Nat Struct Mol Biol 14, 406–412.

Delprato A, Merithew E, Lambright DG (2004). Structure, exchange determinants, and family-wide Rab specificity of the tandem helical bundle and Vps9 domains of Rabex-5. Cell 118, 607–617.

Fukuda M (2002). Synaptotagmin-like protein (Slp) homology domain 1 of Slac2-a/melanophilin is a critical determinant of GTP-dependent specific binding to Rab27A. J Biol Chem 277, 40118–40124.

Fukuda M (2008). Regulation of secretory vesicle traffic by Rab small GTPases. Cell Mol Life Sci 65, 2801–2813.

Fukuda M (2011). TBC proteins: GAPs for mammalian small GTPase Rab? Biosci Rep 31, 159–168.

Fukuda M, Kanno E, Ishibashi K, Itoh T (2008). Large scale screening for novel Rab effectors reveals unexpected broad Rab binding specificity. Mol Cell Proteomics 7, 1031–1042.

Fukuda M, Kanno E, Mikoshiba K (1999). Conserved N-terminal cysteine motif is essential for homo- and heterodimer formation of synaptotagmins III, V, VI, and X. J Biol Chem 274, 31421–31427.

Fukuda M, Mikoshiba K (1999). A novel alternatively spliced variant of synaptotagmin VI lacking a transmembrane domain: implications for distinct functions of the two isoforms. J Biol Chem 274, 31428–31434.

Hattula K, Furuhjelm J, Arffman A, Peränen J (2002). A Rab8-specific GDP/GTP exchange factor is involved in actin remodeling and polarized membrane transport. Mol Biol Cell 13, 3268–3280.

Hutagalung AH, Novick PJ (2011). Role of Rab GTPases in membrane traffic and cell physiology. Physiol Rev 91, 119–149.

Itoh T, Fukuda M (2006). Identification of EPI64 as a GTPase-activating protein specific for Rab27A. J Biol Chem 281, 31823–31831.

Jiménez M, Tsukamoto K, Hearing VJ (1991). Tyrosinases from two different loci are expressed by normal and by transformed melanocytes. J Biol Chem 266, 1147–1156.

Kanno E, Ishibashi K, Kobayashi H, Matsui T, Ohbayashi N, Fukuda M (2010). Comprehensive screening for novel Rab-binding proteins by GST pull-down assay using 60 different mammalian Rabs. Traffic 11, 491–507.

Knödler A, Feng S, Zhang J, Zhang X, Das A, Peränen J, Guo W (2010). Coordination of Rab8 and Rab11 in primary ciliogenesis. Proc Natl Acad Sci USA 107, 6346–6351.

Kuroda TS, Ariga H, Fukuda M (2003). The actin-binding domain of Slac2-a/melanophilin is required for melanosome distribution in melanocytes. Mol Cell Biol 23, 5245–5255.

Kuroda TS, Fukuda M (2004). Rab27A-binding protein Slp2-a is required for peripheral melanosome distribution and elongated cell shape in melanocytes. Nat Cell Biol 6, 1195–1203.

Loftus SK, Larson DM, Baxter LL, Antonellis A, Chen Y, Wu X, Jiang Y, Bittner M, Hammer JA III, Pavan WJ (2002). Mutation of melanosome protein RAB38 in *chocolate* mice. Proc Natl Acad Sci USA 99, 4471–4476.

Ortiz D, Medkova M, Walch-Solimena C, Novick P (2002). Ypt32 recruits the Sec4p guanine nucleotide exchange factor, Sec2p, to secretory vesicles: evidence for a Rab cascade in yeast. J Cell Biol 157, 1005–1015.

Passeron T, Bahadoran P, Bertolotto C, Chiaverini C, Buscà R, Valony G, Bille K, Ortonne JP, Ballotti R (2004). Cyclic AMP promotes a peripheral distribution of melanosomes and stimulates melanophilin/Slac2-a and actin association. FASEB J 18, 989–991.

Pellinen T, Arjonen A, Vuoriluoto K, Kallio K, Fransen JA, Ivaska J (2006). Small GTPase Rab21 regulates cell adhesion and controls endosomal traffic of β1-integrins. J Cell Biol 173, 767–780.

Rink J, Ghigo E, Kalaidzidis Y, Zerial M (2005). Rab conversion as mechanism of progression from early to late endosomes. Cell 122, 735–749.

Rivera-Molina FE, Novick PJ (2009). A Rab GAP cascade defines the boundary between two Rab GTPases on the secretory pathway. Proc Natl Acad Sci USA 106, 14408–14413.

Schwartz SL, Cao C, Pylypenko O, Rak A, Wandinger-Ness A (2007). Rab GTPases at a glance. J Cell Sci 120, 3905–3910.

Sann S, Wang Z, Brown H, Jin Y (2009). Roles of endosomal trafficking in neurite outgrowth and guidance. Trends Cell Biol 19, 317–324.

Seiberg M (2001). Keratinocyte-melanocyte interactions during melanosome transfer. Pigment Cell Res 14, 236–242.

Simpson JC, Griffiths G, Wessling-Resnick M, Fransen JA, Bennett H, Jones AT (2004). A role for the small GTPase Rab21 in the early endocytic pathway. J Cell Sci 117, 6297–6311.

Stenmark H (2009). Rab GTPases as coordinators of vesicle traffic. Nat Rev Mol Cell Biol 10, 513–525.

Tamura K, Ohbayashi N, Ishibashi K, Fukuda M (2011). Structure-function analysis of VPS9-ankyrin-repeat protein (Varp) in the trafficking of tyrosinase-related protein 1 in melanocytes. J Biol Chem 286, 7507–7521.

Tamura K, Ohbayashi N, Maruta Y, Kanno E, Itoh T, Fukuda M (2009). Varp is a novel Rab32/38-binding protein that regulates Tyrp1 trafficking in melanocytes. Mol Biol Cell 20, 2900–2908.

Van Den Bossche K, Naeyaert JM, Lambert J (2006). The quest for the mechanism of melanin transfer. Traffic 7, 769–778.

Wang F, Zhang H, Zhang X, Wang Y, Ren F, Zhang X, Zhai Y, Chang Z (2008). Varp interacts with Rab38 and functions as its potential effector. Biochem Biophys Res Commun 372, 162–167.

Wasmeier C, Romao M, Plowright L, Bennett DC, Raposo G, Seabra MC (2006). Rab38 and Rab32 control post-Golgi trafficking of melanogenic enzymes. J Cell Biol 175, 271–281.

Zhang X, He X, Fu XY, Chang Z (2006). Varp is a Rab21 guanine nucleotide exchange factor and regulates endosome dynamics. J Cell Sci 119, 1053–1062.

Zhu G *et al*. (2007). Structure of the APPL1 BAR-PH domain and characterization of its interaction with Rab5. EMBO J 26, 3484–3493.